

Published in final edited form as:

J Neuroimmunol. 2014 April 15; 269(0): 20–27. doi:10.1016/j.jneuroim.2014.01.013.

Glucocorticoid sensitization of microglia in a genetic mouse model of obesity and diabetes

Aditi Dey^{#1}, Shuai Hao^{#1}, Joanna R. Erion¹, Marlena Wosiski-Kuhn¹, and Alexis M. Stranahan^{1,†}

¹Department of Physiology, Georgia Regents University, Augusta, GA, 30912, USA

These authors contributed equally to this work.

Abstract

db/db mice are a model of obesity and diabetes due to their lack of functional leptin receptors, which leads to insulin resistance, elevated corticosterone levels, and persistent inflammation. Because stress-induced elevations in glucocorticoids sensitize microglia to immune challenges, we hypothesized that corticosteroids might act similarly in the diabetic brain. To test this hypothesis, db/db and wildtype mice were treated with the glucocorticoid synthesis inhibitor metyrapone every day for two weeks. This treatment revealed corticosterone-dependent increases in microglial number and accumulation of the pro-inflammatory cytokines interleukin 1beta and tumor necrosis factor alpha in the hippocampus of db/db mice. Analysis of microglial responses to lipopolysaccharide stimulation revealed that glucocorticoids lower the threshold for release of pro-inflammatory cytokines, underscoring the role of corticosteroids as a precipitating factor for neuroinflammation in obesity and diabetes.

Keywords

obesity; inflammation; hippocampus; corticosterone; glucocorticoid

While there is significant consensus that obesity, and the metabolic consequences of obesity, involves activation of peripheral immune responses (Kanneganti and Dixit, 2012), the extent to which these responses extend to the brain is unclear. Given that the central nervous system is thought to be protected from the circulating immune milieu by the blood-brain barrier, the question of whether neuroinflammation accompanies peripheral immune activation in obesity has received little attention until recently. Several groups have now reported increases in the number and reactivity of microglia, the resident macrophages of the brain, in hypothalamic nuclei that mediate food intake and metabolism (Thaler et al., 2010). However, neural changes in obesity and its endocrine comorbidities are not confined to

© 2014 Elsevier B.V. All rights reserved.

[†]Corresponding author: Alexis M. Stranahan, Medical College of Georgia, Georgia Regents University, Physiology Department, 1120 15th St, room CA3145, Augusta GA 30912, Phone: (706)721-7885, astranahan@gru.edu.

Publisher's Disclaimer: This is a PDF file of an unedited manuscript that has been accepted for publication. As a service to our customers we are providing this early version of the manuscript. The manuscript will undergo copyediting, typesetting, and review of the resulting proof before it is published in its final citable form. Please note that during the production process errors may be discovered which could affect the content, and all legal disclaimers that apply to the journal pertain.

circuits traditionally associated with ingestive behavior and glycemic control. Imaging studies (Falvey et al., 2013) and longitudinal studies of cognition (Xu et al., 2010) have reliably demonstrated structural atrophy in the medial temporal lobe and behavioral impairment on tests of learning and memory in individuals with obesity and diabetes. Although mechanistic data are somewhat scarce, the literature surrounding cognitive and synaptic impairment in rodent models of obesity and diabetes suggests that exposure to chronic elevations in adrenal steroid hormones could contribute to memory deficits (Stranahan et al., 2008a). Taken together, these converging lines of evidence suggest that diabetes and obesity impair cognition, in part by elevating corticosterone levels, but the neuroimmune consequences of manipulating corticosterone have yet to be addressed.

Glucocorticoids are thought to blunt inflammatory responses, based on the consequences of acute exposure to cortisol, corticosterone, and other synthetic corticosteroids. In the context of protracted exposure, such as that which occurs in chronic stress, anti-inflammatory effects are reversed, and glucocorticoids convert from anti-inflammatory to pro-inflammatory (Sorrells et al., 2009). These observations rest primarily on data from studies of psychological stress (Frank et al., 2007) and direct administration of exogenous adrenal steroids (Frank et al., 2012). Given that the endocrine and immune profile in obesity and diabetes differs from that of normoglycemic individuals, the extent to which perturbation of adrenal steroid hormones in obesity and diabetes might elicit central nervous system inflammation in this context remains uncertain.

In these experiments, we used a genetic mouse model of obesity and diabetes arising from leptin receptor deficiency (db/db mice) that exhibits chronically elevated corticosterone levels. db/db mice develop hyperglycemia and insulin resistance during the early postnatal period (Timmers et al., 1986), and also exhibit increased circulating corticosterone concentrations five to six weeks after birth (Takeshita et al., 2000). We administered the corticosterone synthesis inhibitor metyrapone for two weeks, beginning at six weeks of age to prevent the development of hypercortism, and measured levels of pro-inflammatory cytokines in the hippocampus. We quantified hippocampal microglia with unbiased stereology, and assessed microglial reactivity *ex vivo* following LPS stimulation. These analyses revealed that, similar to psychogenic stressors, diabetes and obesity-induced elevations in corticosterone mediate hippocampal neuroinflammation and microgliosis. These effects were accompanied by a lower threshold for induction of pro-inflammatory cytokines following *ex vivo* stimulation of isolated microglia from diabetic mice. Taken together, these observations support a central role for chronically elevated corticosterone levels as a mechanism for neuroinflammation in obesity and diabetes.

Materials and Methods

Animals and drug treatment

Male db/db homozygous mice on the C57Bl6/J background and wildtype C57Bl6/J control mice were obtained from Jackson Laboratories (Bar Harbor, Maine, USA) at five weeks of age. Mice were routinely housed four per cage, with the exception that mice used for assessment of food intake and glucose and insulin metabolism were singly housed. After one week of acclimation to the animal facility, mice were injected with metyrapone (Tocris

Bioscience; 100mg/kg, IP) every day between 8 and 10AM (lights-on at 7AM) to lower and normalize corticosterone levels. This dose was selected on the basis of previous studies using metyrapone to lower corticosterone levels in db/db mice (Takeshita et al., 2000). After fourteen days of treatment with metyrapone or vehicle, (n=8) mice from each genotype and drug condition were prepared for various endpoints as shown in Figure 1A.

Assessment of glucose and insulin metabolism

Glucose and insulin tolerance testing took place between 8 AM and 10AM following an overnight fast. Mice were quickly (<3min) assessed for basal glucose levels using a handheld glucometer (Freestyle Lite), before being injected with 1.0g/kg glucose or 0.25IU/kg insulin. Samples were then measured at specified intervals following glucose or insulin administration. For assessment of the insulin response to glucose challenge, blood draws were conducted via the tail vein at the specified intervals and serum was separated through centrifugation prior to ELISA for quantification of insulin levels as described (Stranahan et al., 2009).

For direct assessment of hippocampal insulin sensitivity, acute slices were prepared from an additional cohort of db/db and wildtype mice treated with metyrapone or vehicle, following an overnight fast, as described for electrophysiology in (Stranahan et al., 2008a). Insulin (Novolog; 100nM in artificial cerebrospinal fluid; ACSF) or vehicle (ACSF alone) was applied to the slices for one hour. The hippocampus was then excised from the slices and frozen at -80C prior to protein extraction and quantification by western blotting.

Immunohistochemistry and unbiased stereology

Labeling for the microglia and macrophage marker ionized calcium binding adapter protein 1 (IBA1) was carried out using standard peroxidase immunohistochemistry. In brief, a 1:3 series of 40 micron sections throughout the rostrocaudal extent of the hippocampus was generated from vehicle- or metyrapone-treated wildtype or db/db mice perfused with 0.4% paraformaldehyde in phosphate buffer (pH=7.5). Sections were blocked in 0.3% hydrogen peroxide in phosphate-buffered saline (PBS) prior to overnight incubation with primary antibody rabbit anti-IBA1 (1:1,000 in PBS; Wako Diagnostics). The following day, sections were washed in PBS, and the bound primary antibody was detected with biotinylated secondary antibody (goat anti-rabbit; 1:500, Vector Labs). After additional washes, the biotin signal was amplified through application of avidin-biotin-horseradish peroxidase using a Vectastain ABC Elite kit. The amplified signal was visualized using diaminobenzadine with nickel enhancement (Vector Labs) and tissue sections were mounted and dried prior to counterstaining with Methyl Green (Sigma-Aldrich). For stereological cell counting, systematic random sampling schemes were implemented with the aid of StereoInvestigator software (Microbrightfield, VT, USA). The XY step size was 300 microns and the square optical disector was 50micron per side. The disector height was 10 microns with a 1.5 micron guard zone. These sampling parameters routinely yielded coefficient of variation values (Gundersen, m=1) that were less than 0.1.

Microglia isolation

Microglia were isolated for ex vivo stimulation experiments by Percoll density gradient as described (Frank et al., 2006), with modifications. Forebrains from mice that had been transcardially perfused with Dulbecco's phosphate-buffered saline (dPBS) were homogenized in a Tenbroeck handheld homogenizer with dPBS supplemented with 2% glucose. The resultant homogenate was passed through a 40 micron cell strainer (BD Bioscience) and briefly centrifuged to pellet the cells. The cell pellet was resuspended in 70% isotonic Percoll, and additional layers of 30% isotonic Percoll and 1× dPBS were applied to create a gradient. The gradients were centrifuged at 1,200×g to separate mononuclear cells from the other CNS elements, and the resulting 70%/30% interface was collected and washed to remove residual Percoll. The wash step involved adding five volumes of dPBS for each volume of cells, prior to mixing by gentle inversion and centrifugation at 1,000×g for 15min. The resulting pellet was resuspended in 100 microliters of RPMI media with 10% heat-inactivated fetal bovine serum (FBS). Ten microliters of the cell suspension was diluted at 1:50 in dPBS for cell counting and morphological analysis using a Scepter instrument (Millipore). For a subset of mice in each condition, ten microliters of cells were stained with Trypan blue (0.5%) and counted by hemacytometer. Cells were then plated at 10,000 cells/well for stimulation with increasing concentrations of lipopolysaccharide (Sigma-Aldrich, catalog #L4391) in RPMI+10%FBS. Incubation with LPS was carried out in a cell culture incubator under 5%CO₂ for eighteen hours, prior to collection of media by aspiration. Media samples were stored at -80C until analysis of interleukin 1beta by ELISA.

Cell viability assay and immunofluorescent analysis of cell markers

Cell viability was assessed using a colorimetric assay kit from R&D Systems (catalog #4891-025-K). This assay measures the cleavage of yellow tetrazolium salts that occurs during mitochondrial electron transport. The cleaved salts form an orange formazan dye and the optical density of the orange dye is proportional to the number of metabolically active cells in each well. The XTT reagent solution was applied to each well after aspiration to collect the media and the plate was incubated for 30min at 37C under 5% CO₂. Following this incubation, the optical density of each well was read at 490nm, with correction at 630nm, using a SpectraMax plate reader (Molecular Devices). Cells that were not previously treated with LPS were used as a reference value to normalize the optical density from wells that received LPS stimulation.

For a subset of animals in each condition, we validated the purity of the cells collected at the 70%/30% interface by immunofluorescent detection of the microglia and macrophage marker IBA1, as well as the astroglial marker glial fibrillary acidic protein (GFAP). Cells were fixed in 4% paraformaldehyde and applied to a well created using a PAP pen on lysine-coated slides. After the fixed cells had dried and adhered to the slide, primary antibodies to IBA1 (rabbit polyclonal, 1:500, Wako Diagnostics) and GFAP (mouse monoclonal, 1:200, Millipore) were applied, and incubated with the slides for 4hr at room temperature in a humidity chamber. Slides were washed, and secondary antibodies (goat anti-rabbit Alexa 488 and goat anti-mouse Alexa 568) were applied at 1:1,000 for 1hr.

Following additional washes, nuclei were counterstained in DAPI prior to imaging on a Zeiss LSM 510 Meta upright confocal microscope.

Enzyme-linked immunosorbent assay

Serum samples were diluted at 1:20 for measurement of insulin (Chrysal Chem) or at 1:100 for measurement of corticosterone (Abcam) levels by ELISA. Dilutions were made in the sample diluent provided with each kit and the assay procedure followed the manufacturer's protocol. Hippocampal protein extraction and quantification of total protein by Bradford assay took place as described (Stranahan et al., 2009). Levels of the proinflammatory cytokines interleukin 1beta and tumor necrosis factor alpha were measured in protein extracts using commercially available ELISA kits from R&D Systems. For measurement of interleukin 1beta, homogenates were diluted 1:10, and for quantification of tumor necrosis factor alpha, undiluted homogenate was applied to wells in duplicate according to the manufacturer's instructions.

Western blotting

For analysis of hippocampal insulin sensitivity, acute hippocampal slices were treated with insulin or ACSF as described above, snap frozen, and stored at -80°C prior to protein extraction and western blotting. Fifty micrograms of extracted protein was loaded and separated through gel electrophoresis. Proteins were then transferred to nitrocellulose membranes, blocked in 5% nonfat milk, and probed with antibodies diluted at 1:1,000 in Tris-buffered saline with Tween-20 and applied overnight at 4°C with shaking. The antibodies were mouse monoclonals directed against insulin receptor beta subunit (IR β ; Millipore), phospho-IR β (Millipore), or β -actin as loading control (Sigma-Aldrich). The secondary antibody was a horseradish peroxidase-conjugated horse anti-mouse from Vector Labs, applied for 1hr at room temperature with shaking, prior to chemiluminescence detection and visualization on a Protein Simple digital documentation system. Band intensities were measured in ImageJ and the phospho-IR β signal was normalized to total IR β for subsequent statistical analysis.

Statistical Analysis

All analyses of a single endpoint utilized 2×2 ANOVA in Graphad Prism 5.0. Repeated measures experiments, including the glucose and insulin tolerance tests, body weight gain, and ex vivo microglia stimulation experiments, were analyzed by 2×2 repeated measures ANOVA using PASW Statistics version 18.0. Bonferonni-corrected post hoc tests were used to compare groups analyzed using 2×2 ANOVA, while Tukey's HSD post hoc was applied to the repeated measures designs. Correlations between cell counts generated using the Scepter instrument (Millipore) and the percent viable cells generated by trypan blue exclusion using a hemacytometer were analyzed using Pearson's correlation. All analyses were conducted with statistical significance set at $p < 0.05$.

Results

Metyrapone partially rescues peripheral glucose and insulin sensitivity in db/db mice

Metyrapone treatment (100mg/kg, IP; Figure 1A) lowers corticosterone levels in db/db mice (for the genotype \times drug interaction following 2×2 ANOVA, $F_{1,20}=18.74$, $p=0.003$; Figure 1B) and induces compensatory adrenal hypertrophy, a recognized physiological response to corticosteroid inhibition (for the main effect of drug treatment following 2×2 ANOVA, $F_{1,20}=7.48$, $p=0.02$; Figure 1C). Because corticosteroid inhibition could potentially impact multiple aspects of metabolic homeostasis (Karatsoreos et al., 2010), we initially assessed food intake, body weight, adiposity, and glycemic control in db/db and wildtype mice treated with metyrapone or vehicle.

Pharmacological inhibition of corticosterone synthesis slightly but significantly reduced body weight in db/db mice (for the drug \times genotype interaction following 2×2 repeated measures ANOVA, $F_{1,48}=8.97$, $p=0.004$; Figure 2A). The weight of the epididymal fat deposit was also significantly reduced by metyrapone treatment (for the drug \times genotype interaction following 2×2 ANOVA, $F_{1,10}=6.17$, $p=0.03$, Figure 2B), suggesting that inhibition of corticosterone synthesis reduces adiposity in db/db mice. These changes occurred despite comparable increases in food intake among db/db mice treated with metyrapone or vehicle (for the effect of genotype following 2×2 ANOVA, $F_{1,48}=14.30$, $p=0.004$; Figure 2C).

Glucose and insulin tolerance testing revealed that targeting glucocorticoids influences glycemic control in db/db mice. Metyrapone significantly reduced fasting glucose levels and improved the response to glucose challenge (for the drug \times genotype interaction following 2×2 repeated measures ANOVA, $F_{1,12}=8.17$, $p=0.01$; Figure 2D). Metyrapone also lowered fasting insulin levels and improved the efficiency of the insulin response to glucose challenge in db/db mice (for the drug \times genotype interaction following 2×2 repeated measures ANOVA, $F_{1,23}=15.74$, $p=0.006$; Figure 2E). Insulin tolerance testing further revealed that the glucose-lowering effects of insulin were improved in db/db mice treated with metyrapone, indicative of improved insulin sensitivity (for the drug \times genotype interaction following 2×2 repeated measures ANOVA, $F_{1,23}=19.66$, $p=0.002$; Figure 2F).

Metyrapone treatment does not influence hippocampal insulin sensitivity

Because pharmacological inhibition of corticosterone synthesis attenuated impairments in peripheral measures of glycemic control, we next evaluated the extent to which metyrapone treatment might influence hippocampal insulin sensitivity. Despite improvements in peripheral insulin sensitivity, metyrapone did not reinstate hippocampal insulin sensitivity in db/db mice. Incubation of hippocampal slices with insulin (100nM) comparably evoked phosphorylation of the insulin receptor in db/db mice, irrespective of glucocorticoid status (for the effect of insulin application following $2 \times 2 \times 2$ ANOVA, $F_{1,32}=9.68$, $p=0.001$; Figure 3A-B). The lack of any change in hippocampal insulin sensitivity was particularly prominent when band intensities were quantified based on percent induction of insulin receptor phosphorylation following insulin application to hippocampal slices (for the interaction between drug and genotype on the percent increase in insulin receptor phosphorylation

following 2×2 ANOVA, $F_{1,16}=0.77$, $p=0.41$; Figure 3C). The absence of any change in insulin-induced phosphorylation of hippocampal insulin receptors in vehicle- and metyrapone-treated db/db mice strongly suggests that lowering corticosterone levels does not impact hippocampal insulin sensitivity.

Corticosteroid inhibition reduces accumulation of proinflammatory cytokines in db/db mice

To determine whether lowering corticosterone levels reduces neuroinflammatory markers in db/db mice, we measured levels of interleukin 1beta (IL1beta) and tumor necrosis factor alpha (TNFalpha) in whole hippocampal homogenates. db/db mice treated with vehicle had higher levels of IL1beta in hippocampal protein extracts (Figure 4A). However, pharmacological inhibition of corticosterone synthesis completely reversed the accumulation of IL1beta in db/db mice (for the interaction between drug and genotype following 2×2 ANOVA, $F_{1,31}=7.34$, $p=0.02$). TNFalpha protein expression was also elevated in a corticosterone-dependent manner in db/db mice (for the interaction between drug and genotype following 2×2 ANOVA, $F_{1,31}=6.36$, $p=0.02$; Figure 4B). Based on these measures, we concluded that lowering corticosterone levels through metyrapone treatment blocks the induction of proinflammatory cytokines in the db/db mouse hippocampus.

Lowering corticosterone levels attenuates microgliosis in db/db mice

db/db mice are leptin receptor deficient throughout their development, which could alter the number of microglia in the hippocampus. To address this possibility, we used unbiased stereology to quantify the number of microglia in the dentate molecular layer and granule cell layer (Figure 5A). db/db mice had more microglia than wildtype mice in the vehicle-treated condition, but metyrapone-treated db/db mice were comparable to wildtype mice, suggesting that inhibiting corticosterone synthesis blocks microgliosis (Figure 5B). This change was detectable in both the dentate molecular layer, where the perforant path synapses are located (Figure 5C; $F_{1,22}=10.49$, $p=0.004$), and in the dentate granule cell layer, where the granule cell somata are located ($F_{1,22}=16.89$, $p=0.005$; Figure 5D). This pattern supports the idea that exposure to chronically elevated corticosterone levels induces microgliosis and neuroinflammation in db/db mice.

Metyrapone treatment prevents increased microglial sensitivity to LPS ex vivo

Chronic exposure to high levels of corticosterone increases microglial sensitivity to immune challenges in the context of stress (Frank et al., 2007), but the extent to which elevated corticosterone levels promote microglial reactivity in obesity and diabetes had not yet been evaluated. To evaluate whether adrenal steroids might create an exaggerated response to immune challenge in diabetes and obesity, we isolated forebrain microglia by density gradient centrifugation and stimulated them with increasing doses of lipopolysaccharide (LPS). Because synthesis and release of IL1beta has previously been used as an indicator of microglial priming by elevated corticosterone (Frank et al., 2010), we measured IL1beta in media collected after 18hr LPS stimulation, and determined cell viability using standard methodology.

The density gradient applied in the current experiments differs from previous work in that we used a 70%/30% gradient, rather than 70%/35% (Nair et al., 2007; Wynne et al., 2010) or the more stringent 70%/50% gradient used by Frank et al. (2006). To validate that the 70%/30% gradient generates viable microglia, we used two strategies for cell phenotyping. First, we stained isolated cells with antibodies against the microglia and macrophage marker IBA1, as well as antibodies against the astroglial marker glial fibrillary acidic protein (GFAP). Cells collected at the 70%/30% interface were routinely IBA1-positive and GFAP-negative, despite robust staining of brain tissue sections using the GFAP antibody (Figure 6A). Second, we used an automated cell counting instrument that generates both cell counts and cell sizes, and were routinely able to differentiate isolated cells from debris on the basis of morphology (Figure 6B). Cell counts determined using this strategy were correlated with cell viability as measured through Trypan Blue exclusion (Figure 6C), suggesting that cells collected at the 70%/30% interface are of either microglial or macrophage origin.

Ex vivo stimulation analyses revealed that exposure to elevated corticosterone levels sensitizes microglia to LPS challenge in obesity and diabetes. Forebrain microglia from vehicle-treated db/db mice exhibit greater reactivity to LPS stimulation, based on their lower threshold for releasing IL1beta into the media ($F_{1,32}=3.70$, $p=0.03$). Microglial sensitization was reversed by corticosterone inhibition, suggesting that elevated corticosterone levels contribute to the lower threshold for IL1beta production in db/db mice (Figure 6D). This difference could not be explained by differential viability of the cells, because analysis of cell viability revealed no differences between groups (Figure 6E). These observations suggest that, similar to psychological stress, diabetes-induced elevations in corticosterone increase microglial reactivity to an immune challenge.

Discussion

Emerging data suggest that glucocorticoids, long considered anti-inflammatory based on their acute effects, may actually elicit inflammation in the central nervous system following prolonged stimulation (Sorrells et al., 2009). This observation is increasingly recognized in the context of psychological stress, but had yet to be explored in the context of obesity and diabetes. Our observations in leptin receptor deficient db/db mice demonstrate that obesity and diabetes are accompanied by hippocampal neuroinflammation, and that pharmacological inhibition of corticosterone synthesis prevents microglial reactivity and accumulation of pro-inflammatory cytokines. These changes underscore the contribution of adrenal steroids as a mechanism for neuroinflammation in obesity and diabetes.

Diabetes and obesity in the db/db mouse model arise from a loss-of-function mutation in the gene encoding the long form of the leptin receptor. While leptin regulates immunity independently of corticosterone (Tilg and Moschen, 2006), the current observations in the current study are likely to be independent of leptin signaling, as pharmacological inhibition of corticosterone would not reverse the loss-of-function mutation that elicits obesity and diabetes in db/db mice. Another alternative hypothesis would suggest that, because systemic inhibition of glucocorticoids improves peripheral glycemic control, the hippocampal changes might be secondary to normalization of insulin levels or sensitivity. This indirect hypothesis was ruled out by measuring hippocampal insulin sensitivity directly, but we

cannot rule out the possible contributions of other gut peptides with known actions in the hippocampus. Because immunity and endocrine systems underlying metabolism are both complex systems, the number of potential contributors at the intersection of these two systems increases exponentially, and data from the current report highlight the important (but not exclusive) role of corticosterone in obesity-induced neuroinflammation.

Corticosterone-mediated accumulation of microglia in the hippocampus was accompanied by elevated levels of IL1beta and TNFalpha, two pro-inflammatory cytokines previously demonstrated to mediate neurological dysfunction following immune challenge (Dantzer et al., 2008) or inescapable stress (Frank et al., 2007). This observation suggests a model in which activated microglia synthesize and release pro-inflammatory cytokines that contribute to the impairment of neuronal plasticity previously reported in genetic (Li et al., 2002; Stranahan et al., 2008a) and diet-induced models of obesity and diabetes (Stranahan et al., 2008b, Jeon et al., 2012). The question of whether elevated corticosterone levels mediate or accelerate neuroinflammation in obesity and diabetes remains uncertain, as pro-inflammatory responses have been reported in the hippocampus of models with drastic elevations in corticosterone, such as db/db mice (Dinel et al., 2011), and in models with more subtle alterations in corticosterone, such as diet-induced obesity (Jeon et al., 2012). Given the clinical literature suggesting that diabetes and obesity represent features of a symptomatic constellation collectively termed the 'metabolic syndrome,' it is possible that the subpopulation of obese diabetics exhibiting elevated adrenal steroid hormones might benefit from more aggressive intervention with anti-inflammatory drugs, relative to the larger population of diabetic individuals without this feature. Along these lines, treatment with synthetic corticosteroids might be counterindicated in the aforementioned population, given the potential for a pro-inflammatory response. However, these implications will require further investigation to more clearly elucidate the locus and mechanism for glucocorticoid-mediated inflammation in animal models of obesity and diabetes.

Acknowledgments

We are grateful to Dr. Matthew Frank for initial training on the microglia isolation technique, and to Dr. Steven Maier for generously allowing a lab visit for this purpose. This work was funded in part by National Institutes of Health Grant K01DK100616 to A.M.S., and by summer fellowships from the Diabetes and Obesity Discovery Institute of Georgia Regents University to A.D. and S.H.

References

- Dantzer R, O'Connor JC, Freund GG, Johnson RW, Kelley KW. From inflammation to sickness and depression: when the immune system subjugates the brain. *Nat Rev Neurosci*. 2008; 9:46–56. [PubMed: 18073775]
- Dinel AL, André C, Aubert A, Ferreira G, Layé S, Castanon N. Cognitive and emotional alterations are related to hippocampal inflammation in a mouse model of metabolic syndrome. *PLoS One*. 2011; 6:e24325. [PubMed: 21949705]
- Falvey CM, Rosano C, Simonsick EM, Harris T, Strotmeyer ES, Satterfield S, Yaffe K, Health ABC Study. Macro- and microstructural magnetic resonance imaging indices associated with diabetes among community-dwelling older adults. *Diabetes Care*. 2013; 36:677–82. [PubMed: 23160721]
- Frank MG, Baratta MV, Sprunger DB, Watkins LR, Maier SF. Microglia serve as a neuroimmune substrate for stress-induced potentiation of CNS pro-inflammatory cytokine responses. *Brain Behav Immun*. 2007; 21:47–59. [PubMed: 16647243]

- Frank MG, Miguel ZD, Watkins LR, Maier SF. Prior exposure to glucocorticoids sensitizes the neuroinflammatory and peripheral inflammatory responses to *E. coli* lipopolysaccharide. *Brain Behav Immun.* 2010; 24:19–30. [PubMed: 19647070]
- Frank MG, Thompson BM, Watkins LR, Maier SF. Glucocorticoids mediate stress-induced priming of microglial pro-inflammatory responses. *Brain Behav Immun.* 2012; 26:337–45. [PubMed: 22041296]
- Frank MG, Wieseler-Frank JL, Watkins LR, Maier SF. Rapid isolation of highly enriched and quiescent microglia from adult rat hippocampus: immunophenotypic and functional characteristics. *J Neurosci Methods.* 2006; 151:121–30. [PubMed: 16125247]
- Jeon BT, Jeong EA, Shin HJ, Lee Y, Lee DH, Kim HJ, Kang SS, Cho GJ, Choi WS, Roh GS. Resveratrol attenuates obesity-associated peripheral and central inflammation and improves memory deficit in mice fed a high-fat diet. *Diabetes.* 2012; 61:1444–54. [PubMed: 22362175]
- Kanneganti TD, Dixit VD. Immunological complications of obesity. *Nat Immunol.* 2012; 13:707–12. [PubMed: 22814340]
- Karatsoreos IN, Bhagat SM, Bowles NP, Weil ZM, Pfaff DW, McEwen BS. Endocrine and physiological changes in response to chronic corticosterone: a potential model of the metabolic syndrome in mouse. *Endocrinology.* 2010; 151:2117–27. [PubMed: 20211972]
- Li XL, Aou S, Oomura Y, Hori N, Fukunaga K, Hori T. Impairment of long-term potentiation and spatial memory in leptin receptor-deficient rodents. *Neuroscience.* 2002; 113:607–15. [PubMed: 12150780]
- Nair A, Hunzeker J, Bonneau RH. Modulation of microglia and CD8(+) T cell activation during the development of stress-induced herpes simplex virus type-1 encephalitis. *Brain Behav Immun.* 2007; 21:791–806. [PubMed: 17349776]
- Sorrells SF, Caso JR, Munhoz CD, Sapolsky RM. The stressed CNS: when glucocorticoids aggravate inflammation. *Neuron.* 2009; 64:33–9. [PubMed: 19840546]
- Stranahan AM, Arumugam TV, Cutler RG, Lee K, Egan JM, Mattson MP. Diabetes impairs hippocampal function through glucocorticoid-mediated effects on new and mature neurons. *Nat Neurosci.* 2008a; 11:309–17. [PubMed: 18278039]
- Stranahan AM, Lee K, Martin B, Maudsley S, Golden E, Cutler RG, Mattson MP. Voluntary exercise and caloric restriction enhance hippocampal dendritic spine density and BDNF levels in diabetic mice. *Hippocampus.* 2009; 19:951–61. [PubMed: 19280661]
- Stranahan AM, Norman ED, Lee K, Cutler RG, Telljohann RS, Egan JM, Mattson MP. Diet-induced insulin resistance impairs hippocampal synaptic plasticity and cognition in middle-aged rats. *Hippocampus.* 2008b; 18:1085–8. [PubMed: 18651634]
- Takeshita N, Yoshino T, Mutoh S. Possible involvement of corticosterone in bone loss of genetically diabetic db/db mice. *Horm Metab Res.* 2000; 32:147–51. [PubMed: 10824711]
- Thaler JP, Choi SJ, Schwartz MW, Wisse BE. Hypothalamic inflammation and energy homeostasis: resolving the paradox. *Front Neuroendocrinol.* 2010; 31:79–84. [PubMed: 19822168]
- Tilg H, Moschen AR. Adipocytokines: mediators linking adipose tissue, inflammation and immunity. *Nat Rev Immunol.* 2006; 6:772–83. [PubMed: 16998510]
- Timmers K, Voyles NR, Zalenski C, Wilkins S, Recant L. Altered beta-endorphin, Met- and Leu-enkephalins, and enkephalin-containing peptides in pancreas and pituitary of genetically obese diabetic (db/db) mice during development of diabetic syndrome. *Diabetes.* 1986; 35:1143–51. [PubMed: 2944783]
- Wynne AM, Henry CJ, Huang Y, Cleland A, Godbout JP. Protracted downregulation of CX3CR1 on microglia of aged mice after lipopolysaccharide challenge. *Brain Behav Immun.* 2010; 24:1190–201. [PubMed: 20570721]
- Xu W, Caracciolo B, Wang HX, Winblad B, Bäckman L, Qiu C, Fratiglioni L. Accelerated progression from mild cognitive impairment to dementia in people with diabetes. *Diabetes.* 2010; 59:2928–35. [PubMed: 20713684]

Research Highlights

- Pharmacological inhibition of corticosterone attenuates microgliosis in db/db mice
- Metyrapone blocks hippocampal cytokine accumulation in db/db mice
- Corticosterone sensitizes microglia to ex vivo immune stimulation in db/db mice

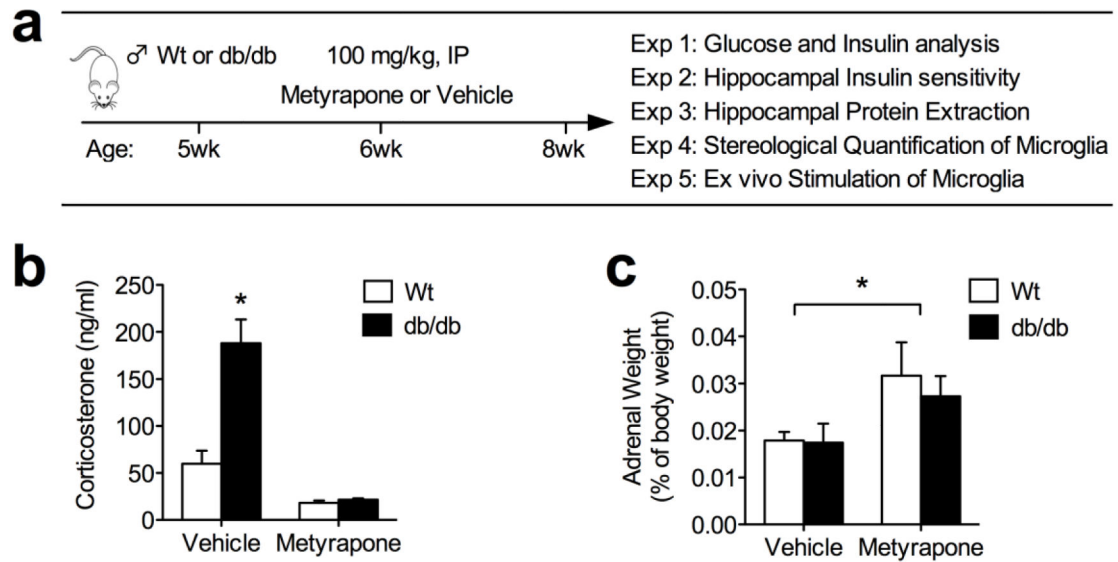


Figure 1. Metyrapone treatment lowers corticosterone levels

(A), Experimental design. (B), Serum corticosterone levels measured two hours after lights-on, demonstrating that treatment with the 11beta hydroxylase inhibitor metyrapone reduces corticosterone levels in db/db mice. (C), Adrenal hypertrophy occurs as a compensatory response following metyrapone treatment, and this physiological effect was detected in mice from the current experiment. For all graphs, asterisk (*) indicates statistical significance at $p < 0.05$ following 2×2 ANOVA, and error bars depict the s.e.m.

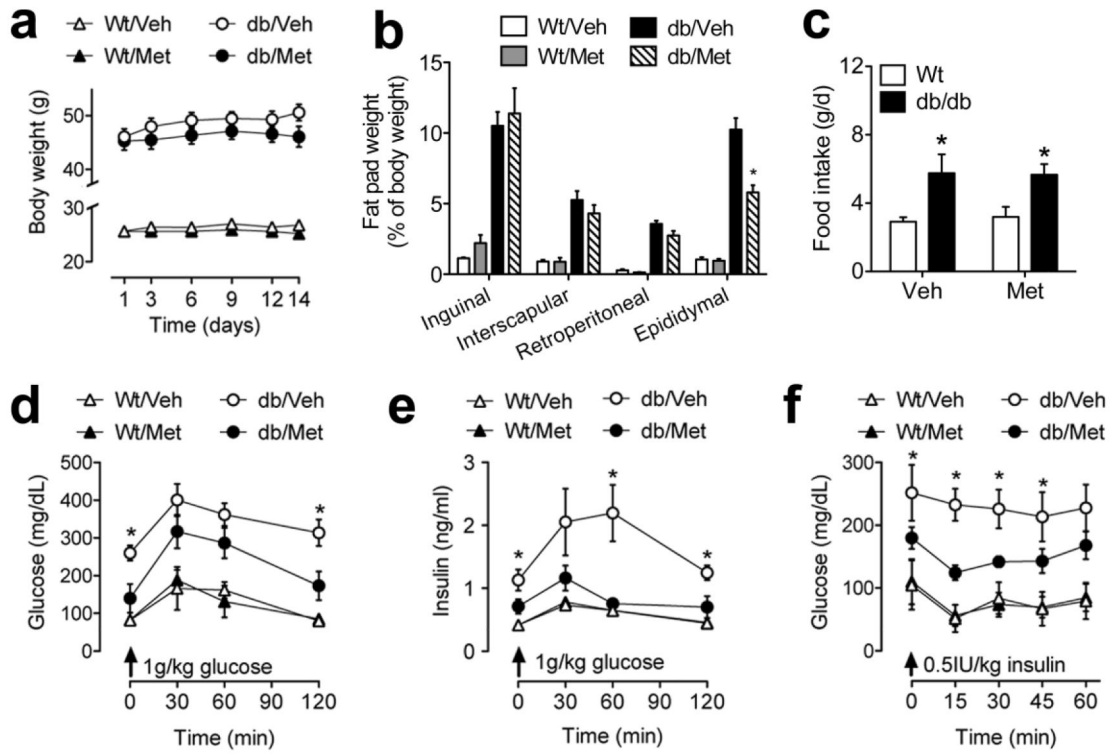


Figure 2. Metrapone treatment reduces body weight and improves glycemic control (A), db/db mice treated with metrapone (db/Met) gained significantly less weight over the fourteen days of treatment, relative to db/db mice treated with vehicle (db/Veh) mice. (B), The weight of the epididymal fat depot is significantly reduced in db/Met mice. (C), Comparable increases in food intake in db/db mice receiving vehicle or metrapone. (D), Glycemic profiles following glucose challenge are improved following metrapone treatment in db/db mice. (E), Insulin responses to glucose challenge are also improved following metrapone treatment in db/db mice. (F), Insulin sensitivity, as measured through insulin tolerance testing, is improved with metrapone administration in db/db mice. For all graphs, asterisk (*) indicates statistical significance at $p < 0.05$ following 2×2 ANOVA (B-C), or 2×2 repeated measures ANOVA (A, D-F) and error bars depict the s.e.m.

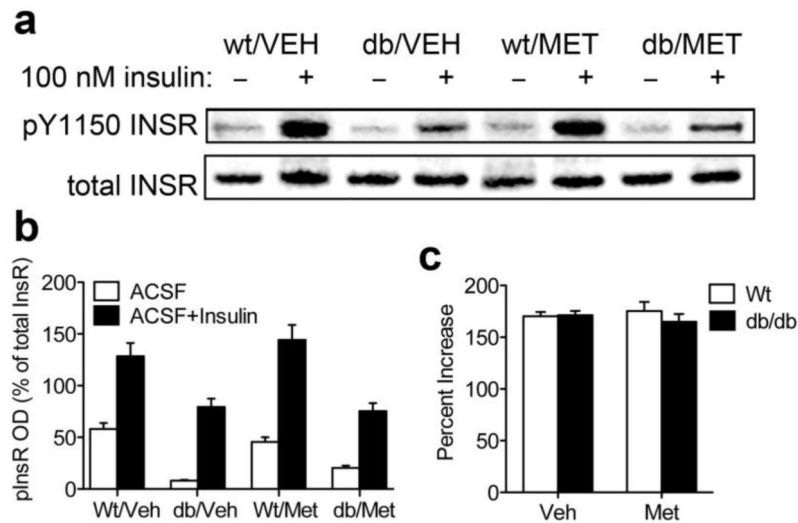


Figure 3. No effect of metyrapone treatment on hippocampal insulin sensitivity

(A), Representative western blot showing insulin-evoked phosphorylation of the insulin receptor at tyrosine 1150 in protein extracts from hippocampal slices generated from mice in the indicated conditions. (B) Incubation of hippocampal slices with insulin (100nM) evoked substantially less phosphorylation of hippocampal insulin receptors in db/db mice, irrespective of glucocorticoid status. For all graphs, asterisk (*) indicates statistical significance at $p < 0.05$ following 2×2 ANOVA, and error bars depict the s.e.m.

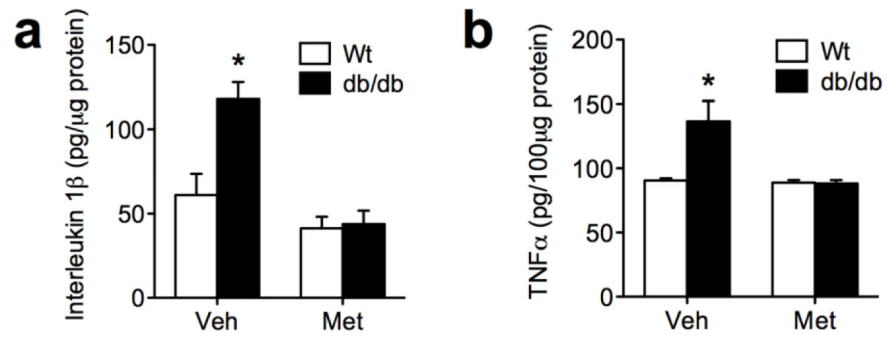


Figure 4. Hippocampal accumulation of proinflammatory cytokines is attenuated by reducing corticosterone levels in db/db mice

(A), Protein expression in interleukin 1beta is elevated in db/db mice treated with vehicle, but not in db/db mice treated with metyrapone. (B), Levels of tumor necrosis factor alpha (TNFalpha) are also increased in a corticosteroid-dependent manner in db/db mice. For all graphs, asterisk (*) indicates statistical significance at $p < 0.05$ following 2×2 ANOVA, and error bars depict the s.e.m.

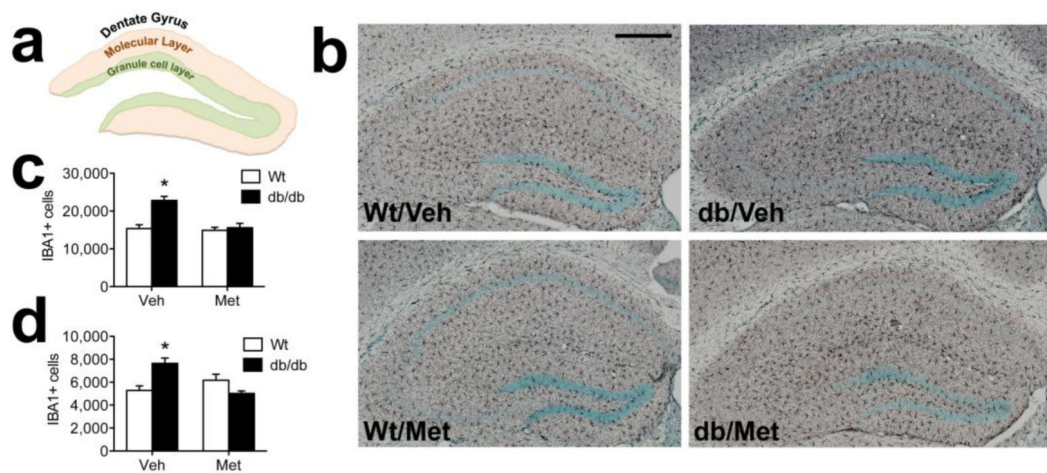


Figure 5. Exposure to elevated corticosterone levels elicits microgliosis in the hippocampal dentate gyrus of db/db mice

(A), Schematic diagram showing regional boundaries of the dentate molecular layer and granule cell layer on a dorsal coronal section through the hippocampus. (B), Micrographs depict labeling for the microglial marker ionized calcium binding adapter protein 1 (Iba1; black staining) in the indicated groups. Scalebar =200 microns. (C), Stereological quantification reveals corticosterone-dependent microgliosis in the dentate molecular layer of the db/db mouse hippocampus. (D), Similar patterns were observed in the granule cell layer, with corticosteroid-dependent increases in microglial numbers observed in db/db mice. For all graphs, asterisk (*) indicates statistical significance at $p < 0.05$ following 2×2 ANOVA, and error bars depict the s.e.m.

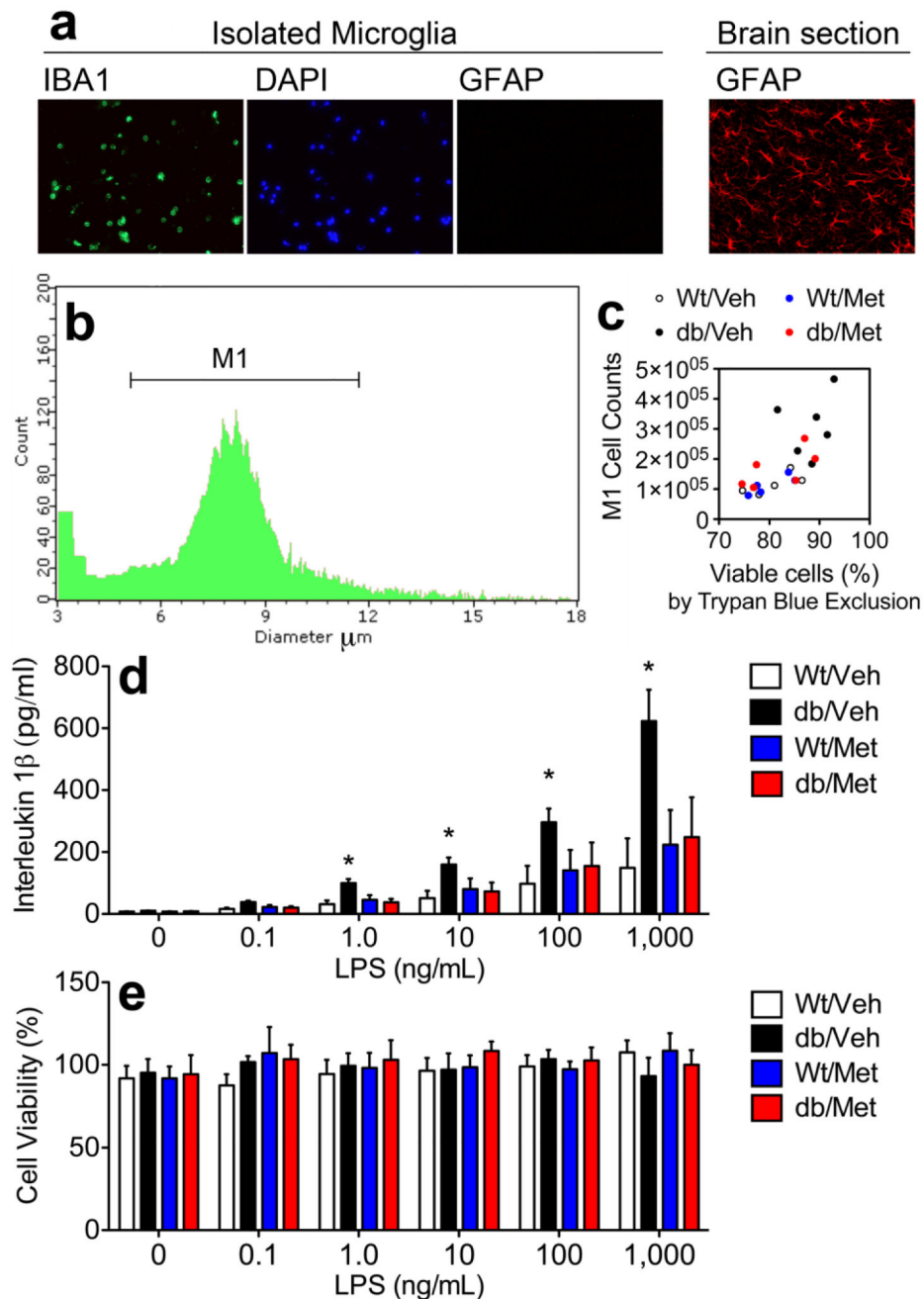


Figure 6. Ex vivo stimulation of microglia reveals corticosteroid-dependent sensitization to an immune challenge in db/db mice

(A), Cells collected at the 70%/30% interface express the microglial marker IBA1, but do not express the astroglial marker GFAP. (B), Automated measurement of cell number and cell diameter easily distinguishes between microglia and debris. (C), Automated cell counts restricted to expected diameter of isolated microglia (M1 region) are positively correlated with cell viability assessed through Trypan Blue exclusion. (D), Levels of the pro-inflammatory cytokine interleukin 1beta were quantified by ELISA in media following 18hr LPS stimulation. Microglia from vehicle-treated db/db mice had a significantly lower

threshold for release of IL1beta, relative to wildtype mice, while microglia from metyrapone-treated db/db mice were indistinguishable from wildtype controls. (E), These patterns could not be explained by differences in cell viability, as analysis of cell viability by XTT assay revealed no differences between groups. For all graphs, asterisk (*) indicates statistical significance at $p < 0.05$ following 2×2 repeated measures ANOVA, and error bars depict the s.e.m.